Desalination and Water Treatment
www.deswater.com

doi: 10.1080/19443994.2015.1046144

57 (2016) 11850–11858
May

Taylor & Francis
Taylor & Francis Group

Adsorption of methyl orange from aqueous solution using chitosan microspheres modified by β-cyclodextrin

Peng Zhao[a], Meihua Xin[b,*], Mingchun Li[b,*], Jun Deng[b]

[a]*College of Chemical Engineering, Huaqiao University, Xiamen, China, Tel. +86 592 6161559; email: zhaopeng@hqu.edu.cn*
[b]*College of Materials Science & Engineering, Huaqiao University, Xiamen, China, Tel. +86 595 22690917; email: mhxin@hqu.edu.cn (M. Xin), Tel. +86 592 6162233; email: mcli@hqu.edu.cn (M. Li), Tel. +86 595 22690819; email: 26847405@qq.com (J. Deng)*

Received 14 August 2014; Accepted 23 April 2015

ABSTRACT

Chitosan microspheres modified by β-cyclodextrin (CDS) were prepared and utilized for removing methyl orange (MO) from aqueous media in this study. Batch experiments were conducted to examine kinetics, adsorption isotherm, pH effect, and thermodynamic parameters. Adsorption data of MO uptake by CDS were analyzed according to Langmuir and Freundlich adsorption models. Thermodynamic parameters for the adsorption system were determinated at 303, 313, 323 and 333 K ($\Delta H^\circ = -26.02$ kJ mol^{-1}; $\Delta G^\circ = -8.66$ to -6.95 kJ mol^{-1} and $\Delta S^\circ = -57.28$ J K^{-1} mol^{-1}). ΔG° values obtained were negative, indicating that the adsorption of MO on the surface of CDS was a spontaneous adsorption process. The kinetics of this process was described very well by a pseudo-second-order rate equation. These results showed that the CDS could be considered as a potential adsorbent for the removal of MO in aqueous solution.

Keywords: Methyl orange; Chitosan microspheres; β-cyclodextrin; Adsorption; Kinetics; Thermodynamics

1. Introduction

Toxic dyes removal from industrial wastewater has become an important issue because of environmental concerns. Some of these dyes are not only aesthetic pollutants, but coloration of water by the dyes may interfere with light penetration affecting aquatic ecosystems [1]. Methyl orange (MO) is widely used in the textile, printing, paper manufacturing, pharmaceutical, food industries and also in research laboratories [2]. MO is toxic, mutagenic and carcinogenic [3,4]. The dye is representative contamination in industrial wastewater. To meet environmental regulations, effluents or water contaminated with MO must be treated before discharge. It is difficult to degrade dye materials because they are very stable to light and oxidation. There are various methods to treat dyes and heavy metal ions from contaminated water, such as ion exchange, adsorption, reverse osmosis, ultrafiltration, oxidation and ozonation [5–10]. Among these methods, adsorption is the most widely used one because of its ease of operation and comparably low cost. The ability of a large variety of adsorbent materials to remove dyes has been proposed and investigated [11,12]. Much attention has recently been focused on

*Corresponding authors.

various biosorbent materials that can be obtained in large quantities and they are harmless to nature. An alternative means of treatment of dyeing wastewater [13–16] has involved chitosan (CS), which is widely distributed and abundant in nature, and is biodegradable [17].

CS is a natural polysaccharide with appealing intrinsic properties, such as biodegradability, biocompatibility, film-forming ability, bioadhesivity, polyfunctionality, hydrophilicity and adsorption properties. These numerous properties lead to the recognition of this polyamine as a promising raw material for adsorption purposes [18]. Most researchers employed CS as adsorbent to treat dyeing wastewater, and had achieved great success. Physically and chemically modified CS has also been used in some works: for example, Wang and Wang employed CS/montmorillonite nanocomposite particles in the sorption of Congo Red, and Lima et al. used CS chemically modified with succinic anhydride for methylene blue adsorption [19,20].

To the authors' knowledge, the use of CS microspheres modified by β-cyclodextrin for removing MO has not been well investigated. The aim of the present study was to investigate and explore the feasibility of CS microspheres modified by β-cyclodextrin for removing MO from aqueous solutions. The influence of several operating parameters for adsorption of MO, such as contact time, temperature and pH, were investigated in batch mode. The kinetic data are fit for different models and the isotherm equilibrium data obey Langmuir and Freundlich.

2. Materials and methods

2.1. Materials and analytical method

All the studies were done using deionized water and reagents of A.R grade. An aqueous stock solution of MO (2,000 mg L^{-1}) was prepared by dissolving MO (molecular formula: $C_{14}H_{14}N_3NaO_3S$, molecular weight: 327.34, Shanghai Sanai Chemical reagent Co. Ltd, China) in deionized water. Other working solutions with different concentration were obtained by successive dilution.

The concentration of the MO solution was analyzed by a UV–visible spectrophotometer (Shimadzu UV-160A) at maximum wave lengths of 465 nm [21].

The adsorbed amount of MO at equilibrium, q_e (mg g^{-1}) was calculated by using the mass balance:

$$q_e = \frac{(C_0 - C_e)V}{W} \quad (1)$$

where V is the solution volume (L), W is the amount of adsorbent (g), and C_0 and C_e are the initial and equilibrium MO a concentrations (mg L^{-1}), respectively.

2.2. Preparation of adsorbents

CS (3.0 g) was dissolved in 50 mL of 2% (w/v) acetic acid solution under stirring at room temperature, then PEG2000 (0.03 g) was added, and the mixture was added to liquid paraffin in a three-necked flask. Span80 (1.5 mL) was added to emulsification for about 0.5 h. Then, 5.7 mL of formaldehyde was added, and the solution was stirred for another 1 h. The reaction solution was poured to the mixture of ethanol/10 wt% NaOH solution. Then cross-linked CS microspheres were suction filtered carefully and washed thoroughly with petroleum ether, anhydrous ethanol and deionized water. Calculated amount of CS microspheres was transferred into a 100 mL three-necked flask with 0.4 mol L^{-1} NaOH solution and 100 mL dimethyl sulfoxide, and then calculated amounts of β-CD and epoxy chloropropane were added to the mixture. The mixture was stirred for 8 h at 60°C. The products were suction filtered carefully and washed thoroughly with acetone and deionized water. Subsequently the products were moved in a 300 mL HCl solution (0.5 mol L^{-1}) for 6 h at 333 K. Finally, the resulting products were thoroughly washed and vacuum-infiltrated with NaOH solution, ethanol, and deionized water, and then vacuum-dried at 45°C to produce CDS microspheres. The synthesis is shown in Fig. 1.

2.3. Characterization of the adsorbents

The scanning electron microscopic (SEM) of CDS were carried out using scanning electron microscopy (Hitachi S-3500N, Hitachi company, JPN). The FTIR spectra of the CDS and CTS were recorded on a FTIR Spectrometer (Nexus 470, Thermo Nicolet, USA) using KBr pellets over the range 4,000–400 cm^{-1}.

2.4. Effect of contact time

The contact time of adsorbent with adsorbate is of great importance in adsorption since contact time depends on the nature of the system used. Adsorption experiments for MO on CDS were carried out as follows: to each of 0.3 g the CDS sample, 120 mL of solution containing 200 mg L^{-1} of MO was added. The samples were shaken at room temperature for periods

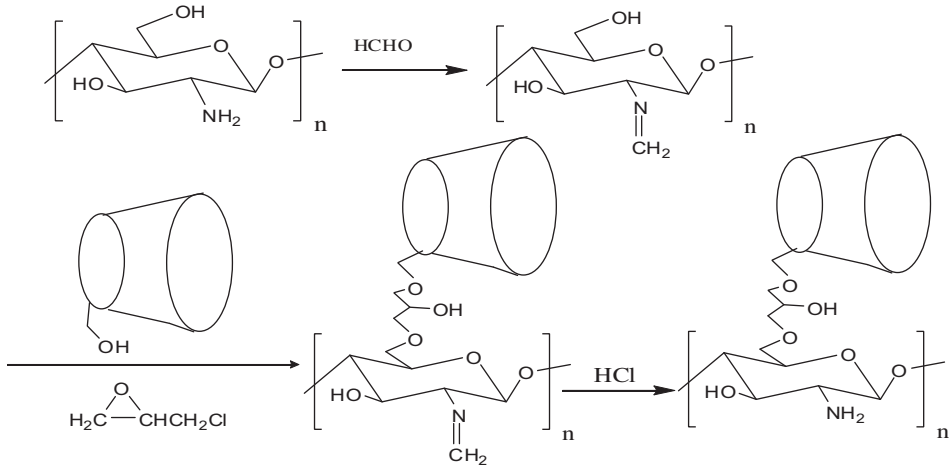

Fig. 1. Scheme for preparation of the modified CS microspheres.

ranging from 5 min to 3 h, and then 5 mL portions of liquid phases were measured.

2.5. Effect of pH

Effect of initial solution pH on adsorption was determined by mixing 0.1 g of CDS with 50 mL of solution containing MO concentration of 100 mg L^{-1} at temperature of 30 ± 1°C and various pH values ranging from 3 to 12. Solution pH was adjusted with 1 M HCl and NaOH solutions. The mixture was shaken for 2 h and the solution was filtered and analysed. Experimental data was the average of triplicate determinations [22].

2.6. The adsorption isotherms

The adsorption isotherms were studied by varying the concentration of MO solutions with a fixed dose of adsorbent. To investigate the sorption isotherms, two models, Langmuir and Freundlich isotherm equations were applied [23,24]. The linearised isotherm equations are expressed as the following:

Langmuir:

$$\frac{C_e}{q_e} = \frac{C_e}{Q_0} + \frac{1}{Q_0 b} \tag{2}$$

Freundlich:

$$\log q_e = \log K + \frac{1}{n}\log C_e \tag{3}$$

where C_e is the equilibrium liquid phase concentration (mg L^{-1}), q_e is the amount of sorbent adsorbed per unit weight (mg g^{-1}); and Q_0 and b are the Langmuir constants related to the sorption capacity and the rate of adsorption, respectively. K and $1/n$ are Freundlich constants. The values of K and $1/n$, which roughly correspond to the adsorption capacity and the heterogeneity factor representing the deviation from linearity of adsorption, respectively.

A further analysis of the Langmuir equation can be made on the basis of a dimensionless equilibrium parameter, R_L [25], also known as the separation factor, given by Eq. (4):

$$R_L = \frac{1}{1 + bC_0} \tag{4}$$

where b (L/mg) is the Langmuir constant and C_0 (mg L^{-1}) is the initial highest concentration of MO. The value of R_L lies between 0 and 1 for a favorable adsorption, while $R_L > 1$ represents an unfavorable adsorption, and $R_L = 1$ represents the linear adsorption, while the adsorption operation is irreversible if $R_L = 0$.

2.7. Thermodynamic studies

Thermodynamic parameters such as free energy (ΔG°), enthalpy (ΔH°), and entropy (ΔS°) change of adsorption can be evaluated from the following equations [26,27]:

$$K_c = \frac{C_{Ae}}{C_e} \tag{5}$$

$$\ln K_c = -\frac{\Delta H^\circ}{RT} + \frac{\Delta S^\circ}{R} \quad (6)$$

where K_c is the equilibrium constant, C_{Ae} is the amount of MO (mg) adsorbed on the adsorbent per liter of the solution at equilibrium, and C_e is the equilibrium concentration (mg L^{-1}) of the MO in the solution. R is the universal gas constant (8.314 J mol^{-1} K) and T is the absolute temperature (in Kelvin). The Gibbs free energy change is related to enthalpy change (ΔH°) and entropy change (ΔS°) at constant temperature by Eq. (7).

$$\Delta G^\circ = \Delta H^\circ - T\Delta S^\circ \quad (7)$$

2.8. Adsorption kinetics

Adsorption kinetics is important from the point of view that it controls the efficiency of the process and the models correlate the adsorbate uptake rate with its bulk concentration. Experiments were also performed in order to understand the kinetics of MO removal by CDS. At various time intervals, samples were taken and the concentration was measured. The amount of MO adsorbed q_t at time t was determined by the following equation:

$$q_t = \frac{(C_0 - C_t)V}{W} \quad (8)$$

where q_t is the amount of MO adsorbed at time t (mg g^{-1}), V is the volume of the solution (L), W (g) is the mass of the adsorbent, C_0 and C_t are the concentrations of the MO at initial ($t = 0$) and at time t, respectively.

In order to analyze the sorption rate, the kinetic data were modeled using Lagergren pseudo-first-order and Ho pseudo-second-order equations [28,29].

Lagergren pseudo-first-order:

$$\log(q_e - q_t) = \log(q_e) - \frac{k_1}{2.303}t \quad (9)$$

Ho pseudo-second-order:

$$\frac{t}{q_t} = \frac{1}{k_2 q_e^2} + \frac{1}{q_e}t \quad (10)$$

where q_t and q_e are the amount of MO adsorbed (mg g^{-1}) at time t and at equilibrium, respectively; k_1 (min^{-1}) and k_2 (mg g^{-1} min^{-1}) are the pseudo-first-order and pseudo-second-order rate constants.

3. Results and discussion

3.1. Sorbent characterization

Fig. 2 shows a general SEM micrograph of the CDS, and it can clearly be seen that the modified CS microspheres are well shaped spheres and have porous surfaces. The CDS have the diameter size range of 35–50 μm. Fig. 3 shows the FT-IR spectra of pure CTS and CDS. Spectrum a retains the characteristic absorption peaks of CTS. The broad bands near 3,449 cm^{-1} indicates the presence of hydroxyl groups and amino groups. The peak at 2,876 cm^{-1} was attributed to the asymmetric stretching of –CH group in the polymer, 1,598 cm^{-1} indicates the amide I group (C–O stretching along the N–H deformation). Compared to CTS, the peak at 3,396 cm^{-1} turns to broad that is attributed to the hydroxyl groups of β-cyclodextrin. The peak at

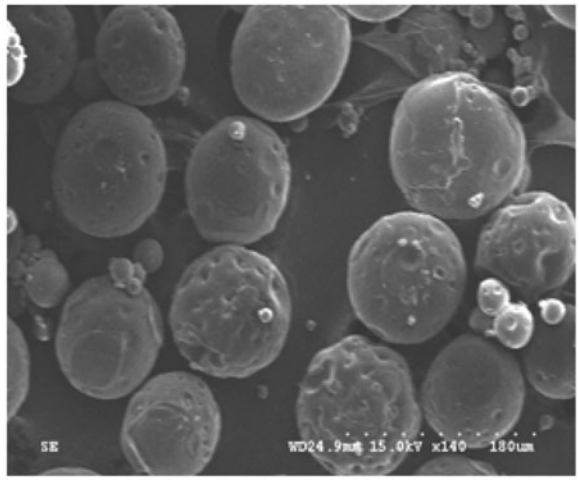

Fig. 2. SEM images of CDS.

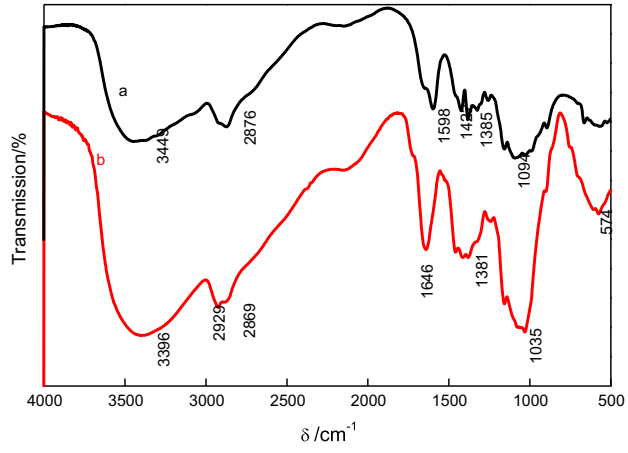

Fig. 3. The FTIR spectra of; (a) CTS; and (b) CDS.

1,646 cm^{-1} is the $N–H_2$ deformation vibration of amino groups. The peak at 1,035 cm^{-1} is assigned to asymmetric –C–O–C– stretching vibration of CDS. The peaks corresponding to hydroxyl, amino and ether groups are shifted indicating CS microspheres modified by β-cyclodextrin. The BET surface area was 2.517 m^2/g. Average pore width was measured 1 μm. Volume of pores were 0.0118 cm^3/g.

3.2. Effect of contact time

The effect of contact time on the adsorption of MO is shown in Fig. 4. Where it is clear that a rapid uptake of MO can be observed within the first 40 min. Thereafter, the adsorption rate decreased, and the adsorption reached equilibrium in about 120 min. The observed removal efficiency was 96.93% at 120 min. The differences in the adsorption values after 120 min were very small. This phenomenon could be attributed to the instantaneous utilization of the most readily available adsorbing sites on the adsorbent surface.

3.3. Effect of pH

Some experiments were carried out to examine the influence of initial pH on the adsorption of MO with 100 mg L^{-1} solutions. The effect of pH on removal of MO dye from aqueous solution at various solution pH is shown in Fig. 5. Accordingly, the percentage of dye removal increased gradually from 75 to 97% with the increase in pH of ranging from 2.1 to 4.4. The low pH leads to an increase in H^+ ions on the CDS surface, that results in strong electrostatic attraction between the negatively charged dye molecules and the positively charged [30]. As the pH of the system increases, there is a decrease in efficiency of the dye removal which could be explained that at high pH, hydroxyl ions can compete with the dye for adsorption sites on the surface of CDS, hence led to a reduction in the percentage of dye removal. In alkaline medium, a small amount of dye is still adsorbed owing to Van der Waals attraction. Moreover, MO can form hydrogen bonds with the OH groups of CS owing to the high electronegativity of its O, N, and S atoms. Below pH 3, a decrease of adsorption, more pronounced with the lowest initial MO concentration, is also observed. Therefore, The optimum pH for the dye removal is 4.4.

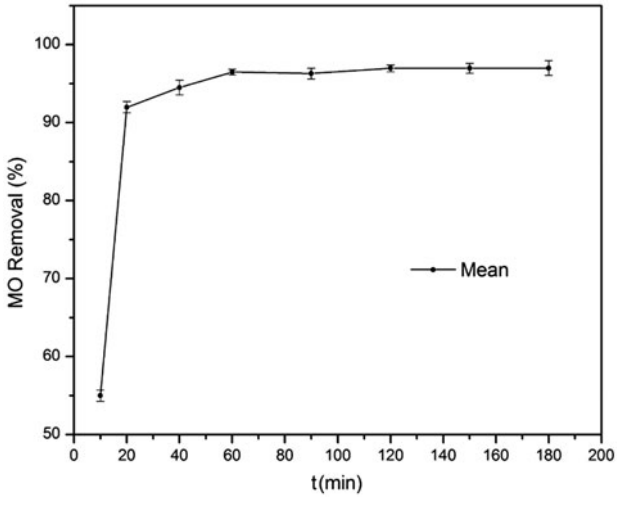

Fig. 4. Effect of contact time on the MO removal.

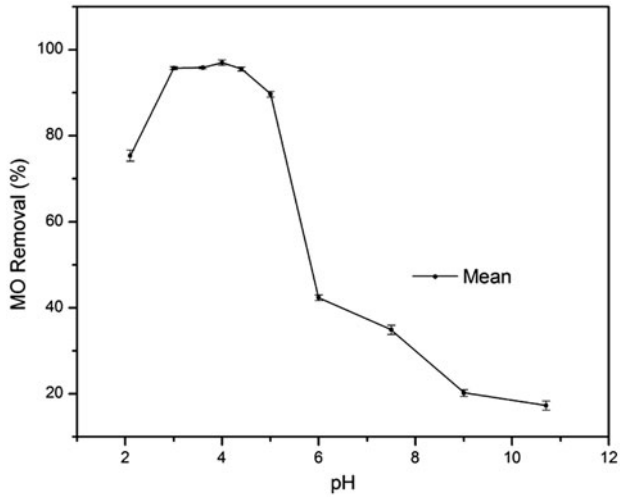

Fig. 5. Influence of initial pH on the MO removal.

3.4. The adsorption isotherm

Isotherms are represented in Figs. 6 and 7, the Langmuir and Freundlich models, respectively. Isotherm parameters for the Langmuir and Freundlich models for the CDS are reported in Table 1. The correlation coefficients (R^2) values were higher for Freundlich isotherm than that of Langmuir isotherm. The high value of correlation coefficient ($R^2 = 0.9992$) reinforces the fact that Freundlich isotherm is more suitable to explain the adsorption of MO from the solution on the current adsorbent. The result is in agreement with the view that the Freundlich model is believed to be the best equilibrium model for molecularly imprinted polymers [31]. The value of n between 1 and 10 indicates favorable adsorption [32], while the relatively low Ka value suggests that a lesser number of active sites are available. The value of R_L in the present investigation is much less than 1 and very close

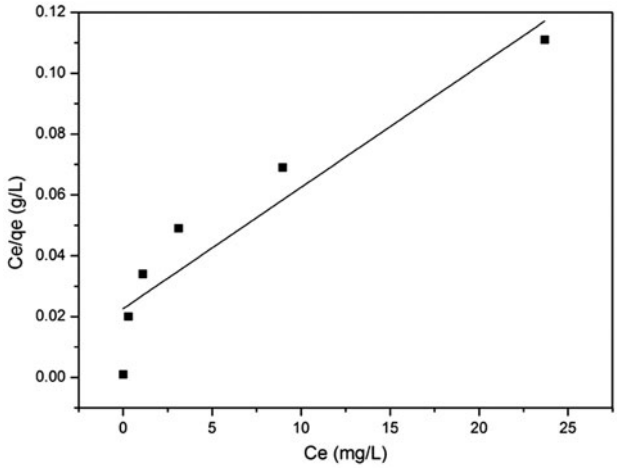

Fig. 6. Langmuir adsorption isotherm for MO adsorption on CDS.

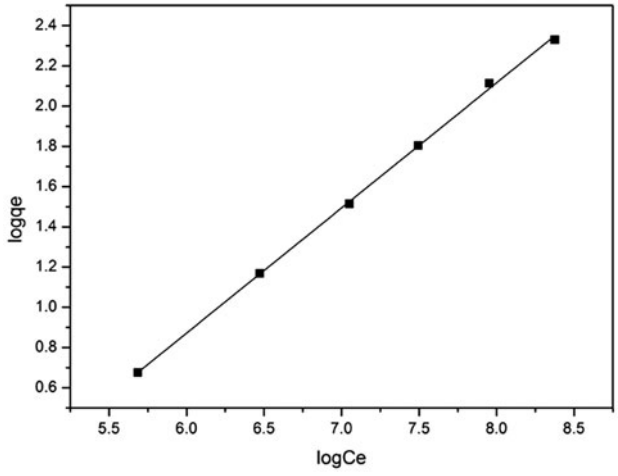

Fig. 7. Freundlich adsorption isotherm for MO adsorption on CDS.

to 0. Therefore, the sorption process is very favorable and the adsorbent employed exhibits a good potential for the removal of MO from aqueous solution.

3.5. Thermodynamic parameters

The values of ΔH° and ΔS° are calculated from the slope and intercept of the Van't Hoff plot (ln K_c vs. $1/T$) shown in Fig. 8. The calculated values are given in Table 2. The negative values of the Gibbs free energy change indicate that the adsorption process is spontaneous. In addition, more negative value with the decrease of temperature shows that the amount adsorbed at equilibrium must decrease with increasing temperature [33]. The negative value of ΔH° (−26.02 kJ mol^{-1}) suggests an exothermic nature of adsorption of MO on the CDS. In other words, the high temperature

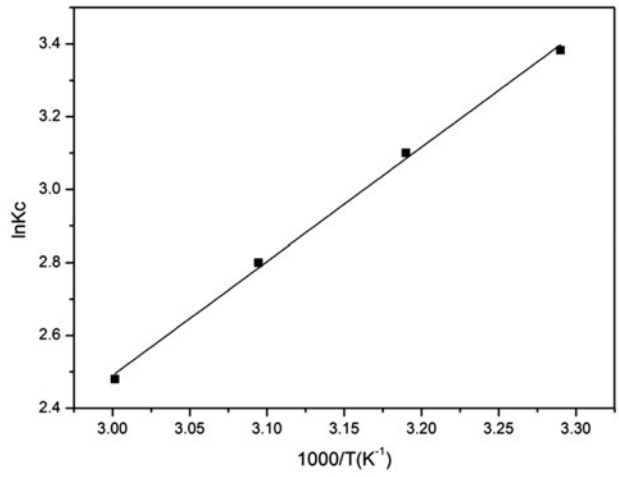

Fig. 8. Plot of log K_c vs. $1/T$ for MO adsorption on CDS.

Table 2
Thermodynamic parameters for adsorption of MO on CDS

Temperature (K)	ΔG° (kJ mol^{-1})	ΔH° (kJ mol^{-1})	ΔS° (J mol^{-1} K^{-1})
303	−8.66	−26.02	−57.28
313	−8.09		
323	−7.52		
333	−6.95		

Table 1
Parameters of the Langmuir and Freundlich isotherm models

	Langmuir				Freundlich		
T (K)	Q_0 (mg g^{-1})	b (L mg^{-1})	R_L	R^2	K (mg g^{-1}) (L mg^{-1})$^{1/n}$	n	R^2
298	250.63	0.177	0.0056	0.8559	0.00138	1.62	0.9992

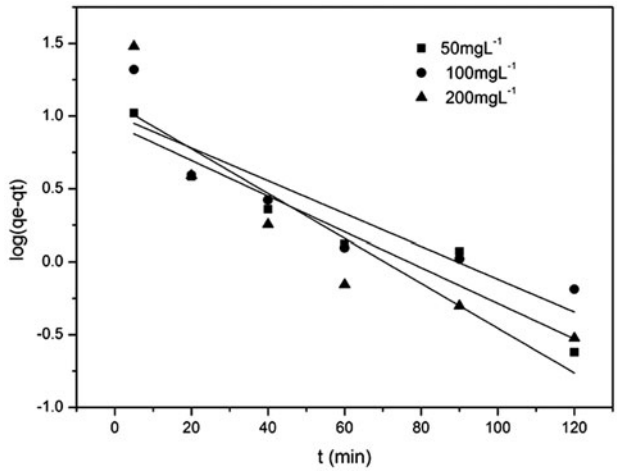

Fig. 9. Lagergren first-order kinetic plot for the sorption of MO on CDS.

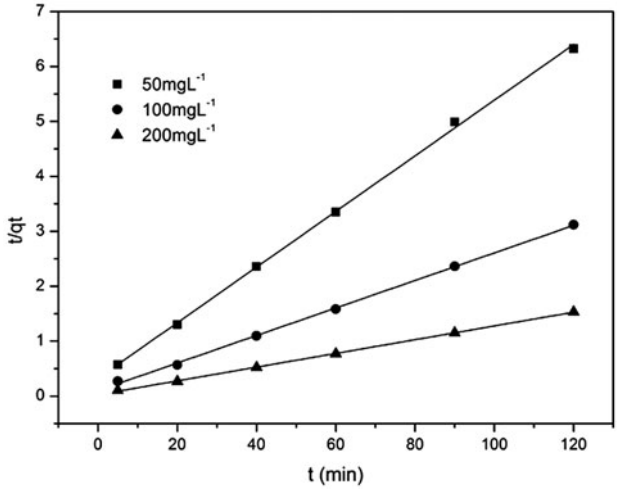

Fig. 10. Second-order kinetic plot for the sorption of MO on CDS.

is unfavorable to the progress of adsorption. The entropy change (ΔS°) was −57.28 J mol^{-1} K^{-1}, the negative value of ΔS° reveals the decreased randomness at the solid/solution interface during the adsorption process. As the free energy changes are negative and accompanied by negative enthalpy changes, the adsorption reactions are spontaneous with a high affinity.

3.6. Adsorption kinetics

For the pepseudo- first-order equation, a plot of log (q_e−q_t) vs. t for sorption of MO is shown in Fig. 9. The application of pseudo-second-order equation by plotting t/q_t vs. t is shown Fig. 10. The kinetic parameters together with correlation coefficients (R^2) have been postulated from the slopes and the intercepts of respective plots and are listed in Table 3. It is important to note that for a pseudo-first-order model, the correlation coefficient is always less than 0.9093 which is indicative of a bad correlation. In contrast, the correlation coefficients for the pseudo-second-order equation were greater than 0.9902 for all concentrations, and the theoretical q_e values obtained from this model is also closer to the experimental $q_{e,exp}$ values at different initial MO concentrations. These results show that the rate of adsorption conforms to pseudo second-order kinetics. Similar results have been observed in the adsorption of MO onto CS/alumina composite [34].

3.7. Comparison with other adsorbents

Finally, a comparison of the maximum MO adsorption capacity on the CDS and some other adsorbents is shown in Table 4. The result indicates the maximum adsorption capacity obtained in this study is higher compared with those obtained from many other adsorbents reported in the literatures. The mechanism of CDS adsorption MO may be as follows: CS molecular structure of the active group; hydrophobic cyclodextrin cavity inclusion of MO effect; specific surface area of the microspheres.

Table 3
Kinetic parameters for pseudo-first order and pseudo-second order

Pseudo-first-order					Pseudo-second-order		
C_0 (mg L^{-1})	$q_{e,exp}$ (mg g^{-1})	K_1 (min^{-1})	q_{e1} (mg g^{-1})	R^2	K_2 (g mg^{-1} min^{-1})	q_{e2} (mg g^{-1})	R^2
50	19.21	0.00282	7.92	0.9093	0.0081	19.61	0.9902
100	39.15	0.00259	8.69	0.7687	0.0062	39.91	0.9997
200	78.60	0.00354	8.80	0.7859	0.0059	80.00	0.9992

Table 4
The adsorptive capacities of various adsorbents for MO

Adsorbent	Q_0 (mg g^{-1})	References
CCM	102.4	[35]
CS/kaolin/γ-Fe_2O_3 nanocomposites	37	[36]
Acid modified carbon coated monolith	147.06	[37]
Calcium alginate/multi-walled carbon	14.13	[38]
Modified silkworm exuviae	87.03	[39]
Maghemite/CS nanocomposite films	29.41	[40]
CDS	250.63	This work

4. Conclusions

CS is a great potential adsorbent for wastewater treatment. In this study, A novel CS microspheres modified by β-cyclodextrin (CDS) has been prepared, characterized and used for the adsorption of MO. The MO adsorption behavior of the prepared CDS has been studied under various conditions of different solution pH values and adsorption contact time. Adsorption equilibrium is attained within a contact time of 120 min. Experimental isotherms of MO are successfully fit to Freundlich isotherms models. The values of ΔH°, ΔS° and ΔG° prove that the adsorption of MO on CDS is an exothermic and a spontaneous process. The adsorption kinetics follows the pseudo-second-order equation for different initial MO concentrations over the whole range studied. The study will be useful for using the novel materials as a low-cost adsorbent for the removal of MO from waste water.

Acknowledgements

This work was financially supported by China Overseas Foundation (Grant No. 11QZR13), The Foundation of Quanzhou city science and technology plan projects (Grant No. 2013Z13).

References

[1] L.H. Ai, C.Y. Zhang, L.Y. Meng, Adsorption of methyl orange from aqueous solution on hydrothermal synthesized Mg–Al layered double hydroxide, J. Chem. Eng. Data 56 (2011) 4217–4225.
[2] S.H. Chen, J. Zhang, C.L. Zhang, Q.Y. Yue, Y. Li, C. Li, Equilibrium and kinetic studies of methyl orange and methyl violet adsorption on activated carbon derived from *Phragmites australis*, Desalination 252 (2010) 149–156.
[3] G.K. Parshetti, A.A. Telke, D.C. Kalyani, S.P. Govindwar, Decolorization and detoxification of sulfonated azo dye methyl orange by *Kocuria rosea* MTCC 1532, J. Hazard. Mater. 176 (2010) 503–509.
[4] N. Mathur, P. Bhatnagar, P. Sharma, Review of the mutagenicity of textile dye products, Univ. J. Environ. Res. Technol. 2 (2012) 1–18.
[5] J.R. Baseri, P.N. Palanisamy, P. Sivakumar, Polyaniline nano composite for the adsorption of reactive dye from aqueous solutions: Equilibrium and kinetic studies, Asian J. Chem. 25 (2013) 4145–4149.
[6] S. Kiran, S. Ali, M. Asgher, Degradation and mineralization of azo dye reactive blue 222 by sequential photo-Fenton's oxidation followed by aerobic biological treatment using white rot fungi, Bull. Environ. Contam. Toxicol. 90 (2013) 208–215.
[7] S.K. Nataraj, K.M. Hosamani, T.M. Aminabhavi, Nanofiltration and reverse osmosis thin film composite membrane module for the removal of dye and salts from the simulated mixtures, Desalination 249 (2009) 12–17.
[8] G. Sheng, H. Dong, Y. Li, Characterization of diatomite and its application for the retention of radiocobalt: Role of environmental parameters, J. Environ. Radioact. 113(113) (2012) 108–115.
[9] G. Sheng, R. Shen, H. Dong, Y. Li, Colloidal diatomite, radionickel, and humic substance interaction: A combined batch, XPS, and EXAFS investigation, Environ. Sci. Pollut. Res. Int. 20 (2013) 3708–3717.
[10] G. Sheng, L. Ye, Y. Li, H. Dong, H. Li, X. Gao, Y. Huang, EXAFS study of the interfacial interaction of nickel (II) on titanate nanotubes: Role of contact time, pH and humic substances, Chem. Eng. J. 248 (2014) 71–78.
[11] M. Auta, B.H. Hameed, Coalesced chitosan activated carbon composite for batch and fixed-bed adsorption of cationic and anionic dyes, Colloids Surf., B 105 (2013) 199–206.
[12] S. Nethaji, A. Sivasamy, A.B. Mandal, Adsorption isotherms, kinetics and mechanism for the adsorption of cationic and anionic dyes onto carbonaceous particles prepared from *Juglans regia* shell biomass, Int. J. Environ. Sci. Technol. 10 (2013) 231–242.
[13] G.Z. Kyzas, M. Kostoglou, A.A. Vassiliou, N.K. Lazaridis, Treatment of real effluents from dyeing reactor: Experimental and modeling approach by adsorption onto chitosan, Chem. Eng. J. 168 (2011) 577–585.
[14] T.Y. Liu, L. Zhao, Z.L. Wang, Removal of hexavalent chromium from wastewater by Fe 0 -nanoparticles-chitosan composite beads: Characterization, kinetics and thermodynamics, Water Sci. Technol. 66 (2012) 1044–1051.

[15] B.H. Guan, W.M. Ni, Z.B. Wu, Y. Lai, Removal of Mn (II) and Zn (II) ions from flue gas desulfurization wastewater with water-soluble chitosan, Sep. Purif. Technol. 65 (2009) 269–274.
[16] M. Visa, A.M. Chelaru, Hydrothermally modified fly ash for heavy metals and dyes removal in advanced wastewater treatment, Appl. Surf. Sci. 303 (2014) 14–22.
[17] P. He, S.S. Davisa, L. Illum, Chitosan microspheres prepared by spray drying, Int. J. Pharm. 187 (1999) 53–65.
[18] C.M. Futalan, C.C. Kan, M.L. Dalida, K.J. Hsien, C. Pascua, M.W. Wan, Comparative and competitive adsorption of copper, lead, and nickel using chitosan immobilized on bentonite, Carbohydr. Polym. 83 (2011) 528–536.
[19] L. Wang, A.Q. Wang, Adsorption characteristics of Congo Red onto the chitosan/montmorillonite nanocomposite, J. Hazard. Mater. 147 (2007) 979–985.
[20] I.S. Lima, E.S. Ribeiro, C. Airoldi, The use of chemical modified chitosam with succinic anhydride in the methylene blue adsorption, Quim. Nova 29 (2006) 501–506.
[21] Q.L. Ma, F.F. Shen, X.F. Lu, W.R. Bao, H.Z. Ma, Studies on the adsorption behavior of methyl orange from dye wastewater onto activated clay, Desalin. Water Treat. 51 (2013) 3700–3709.
[22] G. Sheng, Y. Li, H. Dong, D. Shao, Environmental condition effects on radionuclide 64Cu (II) sequestration to a novel composite: Polyaniline grafted multiwalled carbon nanotubes, J. Radioanal. Nucl. Chem. 293 (2012) 797–806.
[23] I. Langmuir, The constitution and fundamental properties of solids and liquids. Part I. solids, J. Am. Chem. Soc. 38 (1916) 2221–2295.
[24] H. Freundlich, Uber die adsorption in losungen, Zeitsch. Phys. Chem. 57 (1906) 385–470.
[25] K.R. Hall, L.C. Eagleton, A. Acrivos, T. Vermeulen, Pore- and solid-diffusion kinetics in fixed-bed adsorption under constant-pattern conditions, Ind. Eng. Chem. Fundam. 5 (1966) 212–223.
[26] Y.S. Ho, Removal of copper ions from aqueous solution by tree fern, Water Res. 37 (2003) 2323–2330.
[27] K.K. Singh, A.K. Singh, S.H. Hasan, Low cost biosorbent 'wheat bran' for the removal of cadmium from wastewater: Kinetic and equilibrium studies, Bioresour. Technol. 97 (2006) 994–1001.
[28] W. Rudzinski, W. Plazinski, Kinetics of solute adsorption at solid/solution interfaces: A theoretical development of the empirical pseudo-first and pseudo second order kinetic rate equations, based on applying the statistical rate theory of interfacial transport, J. Phys. Chem. B 110 (2006) 16514–16525.
[29] Y.S. Ho, G. Mckay, The kinetics of sorption of divalent metal ions onto sphagnum moss peat, Water Res. 34 (2000) 735–742.
[30] Y.S. Al-Degs, M.I. El-Barghouthi, A.H. El-Sheikh, G.A. Walker, Effect of solution pH, ionic strength, and temperature on adsorption behavior of reactive dyes on activated carbon, Dyes Pigm. 77 (2008) 16–23.
[31] A.M. Rampey, R.J. Umpleby, G.T. Rushton, J.C. Iseman, R.N. Shah, K.D. Shimizu, K.D. Shimizu, Characterization of the imprint effect and the influence of imprinting conditions on affinity, capacity, and heterogeneity in molecularly imprinted polymers using the Freundlich isotherm-affinity distribution analysis, Anal. Chem. 76 (2004) 1123–1133.
[32] S. Arfaoui, N. Frini-Srasra, E. Srasra, Modelling of the adsorption of the chromium ion by modified clays, Desalination 222 (2008) 474–481.
[33] A.K. Meena, G.K. Mishra, P.K. Rai, C. Rajagopal, P.N. Nagar, Removal of heavy metal ions from aqueous solutions using carbon aerogel as an adsorbent, J. Hazard. Mater. 122 (2005) 161–170.
[34] J.X. Zhang, Q.X. Zhou, L.L. Ou, Kinetic, isotherm, and thermodynamic studies of the adsorption of methyl orange from aqueous solution by chitosan/alumina composite, J. Chem. Eng. Data 57 (2012) 412–419.
[35] S. Hosseini, M.A. Khan, M.R. Malekbala, W. Cheah, T.S.Y. Choong, Carbon coated monolith, a mesoporous material for the removal of methyl orange from aqueous phase: Adsorption and desorption studies, Chem. Eng. J. 171 (2011) 1124–1131.
[36] R. Jiang, H. Zhu, Y. Fu, Equilibrium and kinetic studies on adsorption of methyl orange from aqueous solution on chitosan/kaolin/γ-Fe_2O_3 nanocomposite, in: International Conference on Remote Sensing, Environment Transport, Nanjing, vol. 24 (2011) 7565–7568.
[37] W. Cheah, S. Hosseini, M.A. Khan, T.G. Chuah, T.S.Y. Choong, Acid modified carbon coated monolith for methyl orange adsorption, Chem. Eng. J. 215–216 (2013) 747–754.
[38] Y. Li, K. Sui, R. Liu, X. Zhao, Y. Zhang, H. Liang, Y. Xia, Removal of methyl orange from aqueous solution by calcium alginate/multi-walled carbon nanotubes composite fibers, Eng. Proc. 16 (2012) 863–868.
[39] H. Chen, J. Zhao, J. Wu, G. Dai, Isotherm, thermodynamic, kinetics and adsorption mechanism studies of methyl orange by surfactant modified silkworm exuviae, J. Hazard. Mater. 192 (2011) 246–254.
[40] R. Jiang, Y.-Q. Fu, H.-Y. Zhu, J. Yao, L. Xiao, Removal of methyl orange from aqueous solutions by magnetic maghemite/chitosan nanocomposite films: Adsorption kinetics and equilibrium, J. Appl. Polym. Sci. 125 (2012) E540–E549.